Human Molecular Genetics, 2025, Vol. 34, 8, 711–725
https://doi.org/10.1093/hmg/ddae195
Advance access publication date 3 February 2025
Original Article

Decomposing the genetic background of chronic back pain

Elizaveta E. Elgaeva[1,2,*], Irina V. Zorkoltseva[1], Arina V. Nostaeva[2], Dmitrii A. Verzun[1,2], Evgeny S. Tiys[1], Anna N. Timoshchuk[3,4], Anatoliy V. Kirichenko[1], Gulnara R. Svishcheva[1,5], Maxim B. Freidin[6], Frances M. K. Williams[6], Pradeep Suri[7,8], Yurii S. Aulchenko[1,9], Tatiana I. Axenovich[1], Yakov A. Tsepilov[1]

[1]Institute of Cytology and Genetics, Siberian Branch of Russian Academy of Sciences, 10, Ac. Lavrentieva ave., 630090, Novosibirsk, Russia
[2]Novosibirsk State University, 1, Pirogova str., 630090, Novosibirsk, Russia
[3]MSU Institute for Artificial Intelligence, Lomonosov Moscow State University, 27, building 1, Lomonosovsky ave., 119991, Moscow, Russia
[4]Moscow Institute of Physics and Technology, 9, Institutsky lane, 141700, Dolgoprudny, Russia
[5]Vavilov Institute of General Genetics, RAS, 3, Gubkin str., 119991, Moscow, Russia
[6]Department of Twin Research and Genetic Epidemiology, School of Life Course Sciences, King's College London, Westminster Bridge Rd., SE1 7EH, London, UK
[7]Department of Rehabilitation Medicine, University of Washington, 325, Ninth ave., WA 98104, Seattle, USA
[8]VA Puget Sound Health Care System, 1660, South Columbian Way, WA 98108, Seattle, USA
[9]PolyOmica, 61, Het Vlaggeschip, 5237 PA, 's-Hertogenbosch, The Netherlands

[*]Corresponding author. 10, Ac. Lavrentieva ave., Novosibirsk 630090, Russia. E-mail: elizabeth.elgaeva@gmail.com

Abstract

Chronic back pain (CBP) is a disabling condition with a lifetime prevalence of 40% and a substantial socioeconomic burden. Because of the high heterogeneity of CBP, subphenotyping may help to improve prediction and support personalized treatment of CBP. To investigate CBP subphenotypes, we decomposed its genetic background into a shared one common to other chronic pain conditions (back, neck, hip, knee, stomach, and head pain) and unshared genetic background specific to CBP. We identified and replicated 18 genes with shared impact across different chronic pain conditions and two genes that were specific for CBP. Among people with CBP, we demonstrated that polygenic risk scores accounting for the shared and unshared genetic backgrounds of CBP may underpin different CBP subphenotypes. These subphenotypes are characterized by varying genetic predisposition to diverse medical conditions and interventions such as diabetes mellitus, myocardial infarction, diagnostic endoscopic procedures, and surgery involving muscles, bones, and joints.

Keywords: genome-wide association study; shared genetic background; subphenotyping; polygenic risk score; low back pain

Introduction

Back pain is a prevalent clinical syndrome which affects about 40% of the population [1]. It has tremendous social and economic consequences: according to the Global Burden of Disease Study 2016, back pain has been a major cause of disability worldwide for 30 years [2]. Back pain is not only highly prevalent, but it is also difficult to treat [3]. One potential cause of this problem is the high heterogeneity of the condition. Patients with a specific back pain "subphenotype"—a set of common features, distinguishing them from other patients with back pain [4]—may respond to treatment in a different way than a patient of another back pain subphenotype, decreasing the effectiveness of treatment approaches when not tailored to subphenotype. Generic treatment approaches may contribute to back pain patient care costs, which reach 1/5 of total health care costs in a separate country [5]. Subphenotyping may help to more accurately select treatment for patients with back pain and thus decrease these costs.

In 10% of cases acute back pain ceases to be just a symptom and becomes a chronic condition [6]. While the initial cause of acute pain may resolve, an alternative pathophysiological process takes over, leading to anatomical changes and affecting human behavior and mental state [7–9]. Chronic back pain (CBP) has been shown to be a complex trait with heritability estimated between 30 and 68% [10–12]. Genome-wide association studies (GWAS) of chronic pain including but not limited to CBP have revealed about three dozen associated loci [12–17], but only a few of them have been replicated in independent samples.

Studies have demonstrated the presence of a shared genetic background of chronic pain across different pain sites [16, 18, 19]. This shared genetic background is thought to condition the generation, transduction and processing of pain stimuli in general [16]. At the same time, it is reasonable to expect the existence of unshared genetic background specific to chronic back pain (CBP) and related to local pathological processes in the back and spine (e. g. through SOX5 gene [15]), but this has been little studied. Genetic variants related to unshared genetic background of CBP may suggest promising drug targets and biomarkers for diagnosis and treatment of CBP precisely, while the shared genes could be of interest to understand general pain biology and hence contribute in future development of drugs to treat pain irrespective of its site. Therefore, the decomposition of genetic background into

Received: July 4, 2024. **Revised:** October 9, 2024. **Accepted:** December 16, 2024

shared and unshared may be helpful for subphenotyping and personalizing treatment.

Many prior attempts to identify subphenotypes of back pain have been made. Existing approaches to do this classify patients based on observable clinical characteristics, such as pain-related, social, physiological and anatomic features [20], and some of these studies show the utility of this approach for revealing clusters of patients with specific pain trajectories and differentially reacting to treatment [21, 22]. A novel and alternative approach is to subphenotype CBP using genotypic information, which is increasingly available in clinical care and commercial use [23]. Polygenic risk scores (PRS) use GWAS data to estimate the personal genetic liability to disease based on an individual's genotype. In medicine, PRSs have been used to predict disease, however, this information can also be utilized for subphenotyping. While existing chronic back pain PRS models show modest prediction ability [24], division of CBP genetic background into shared and unshared, followed by PRS calculation for each of them, may result in higher statistical power and provide useful information for patients' subphenotyping. To estimate the potential of genetic background decomposition for subphenotyping, a comprehensive examination of the features of shared and unshared genetic background is required.

Previously, we have studied the shared genetic background of chronic musculoskeletal pain at different sites (back, neck, hip, knee) by applying principal component analysis of these traits [16]. We interpreted the first genetically independent phenotype (GIP1, or simply the first principal component) as an approximation of shared genetic background across the considered pain types. In our recent study we developed the novel SHAHER framework [25], allowing more accurate decomposition of genetic background of correlated traits in order to evaluate not only their shared, but unshared genetic factors as well. Here we aimed to employ SHAHER to investigate the complex genetic architecture of CBP by analyzing its shared genetic background across several chronic musculoskeletal and non-musculoskeletal pain conditions (back, neck, hip, knee, stomach and head pain) and its unshared genetic background, particular to chronic pain in the back. We conducted an extensive bioinformatic annotation of shared and unshared genetic background of CBP to reveal functional differences and identify genes associated with each aspect. To find the associated genes, we additionally performed a gene-based association analysis. Finally, we performed a set of PRS analyses among people with CBP to check whether the division between shared and unshared genetic background might be beneficial for CBP subphenotyping.

Results

Overview of the study design

This study was carried out using the results of genome-wide association studies (GWAS) for six chronic pain sites (pain in the back, neck, hip, knee, stomach, and headache). All data ($N_{total} = 456\,000$) were provided by UK Biobank under projects #18219 and #59345. The sample was split into discovery (265 000 individuals of European descent) and replication (a total of 191 000 individuals in three subsamples of African, South Asian and European descent) samples. Details of the phenotypes definition are available in Supplementary Methods. Sample characteristics (size, sex and age structure, pain type prevalence and BMI distribution) are provided in Supplementary Table ST1.

The study design included four stages. In the first stage, we decomposed the genetic background of CBP into shared and unshared ones, and calculated the GWAS summary statistics for two new traits: SGIT (shared genetic impact trait) which is controlled predominantly by shared genetic background common for all traits analyzed, and UGIT (unshared genetic impact trait) which is controlled by genetic background specific for CBP. These calculations were performed for each subsample using the SHAHER framework (Fig. 1, Materials and Methods). Then we performed two meta-analyses for SGIT and UGIT using inverse-variance-weighted method: one combining the summary statistics from the two European samples (European meta-analysis) and another one combining summary statistics from the three replication samples (Replication meta-analysis). Thus, four sets of GWAS summary statistics both for SGIT and UGIT were obtained in the first stage: the "Discovery sample", the "European replication sample", the "European meta-analysis" and the "Replication meta-analysis" (Fig. 1).

In the second stage, we identified loci and genes associated with SGIT and UGIT. We did this using two approaches. The first approach (Fig. 2) was identification of associated loci in the discovery sample, followed by selection of independent association signals within these loci utilizing conditional analysis. For those loci that were previously observed and replicated in our recent work utilizing the same data [15, 16], we did not perform additional analyses. For other association signals, we conducted replication using the Replication meta-analysis. For loci replicated in the Replication meta-analysis we carried out gene prioritization procedure using the European meta-analysis. Gene prioritization included prediction of SNP effects in replicated loci (VEP and FATHMM), analysis of colocalization with gene expression effects (SMR-HEIDI), and gene prioritization using DEPICT and FUMA. Details are available in Supplementary Methods. The second approach utilizing which we identified genetic factors associated with shared and unshared backgrounds of CBP (Fig. 2) was a gene-based association analysis (SKAT-O [26], PCA [27], ACAT-V [28], and ACAT-O [28] methods) using the GWAS summary statistics obtained from the discovery sample, followed by a conditional analysis and replication utilizing the gene-based association analysis results from the European replication sample and European meta-analysis (Fig. 2, Materials and Methods).

At the third stage (Fig. 3), we investigated the genetic architecture of CBP using functional bioinformatic analyses. We conducted a gene set and cell type/tissue enrichment analyses of the identified genes and SNPs in the associated loci in order to characterize the shared and unshared genetic background of CBP. Using GWAS summary statistics obtained for SGIT and UGIT, we estimated the genetic correlations of these traits with a large number of complex human traits from the GWAS-MAP database [29, 30]. Then we calculated polygenic risk scores (PRS) of SGIT and UGIT using individual genotype data and estimated their role in disease/medical intervention prediction.

Finally, we investigated the potential of SGIT and UGIT PRSs for CBP subphenotyping (Fig. 3, Materials and Methods) using participants with CBP from the entire European sample (not divided into discovery and replication). We built binary-coded PRSs for SGIT and UGIT by splitting the PRS distribution into two parts according to the lowest or highest decile (see Materials and Methods). Then we tested if the binary-coded PRSs can be used for CBP subphenotyping.

Decomposition of genetic background of CBP

We estimated the heritability, the genetic correlation and phenotypic correlation for six chronic pain traits from the discovery sample (see Supplementary Methods and Supplementary

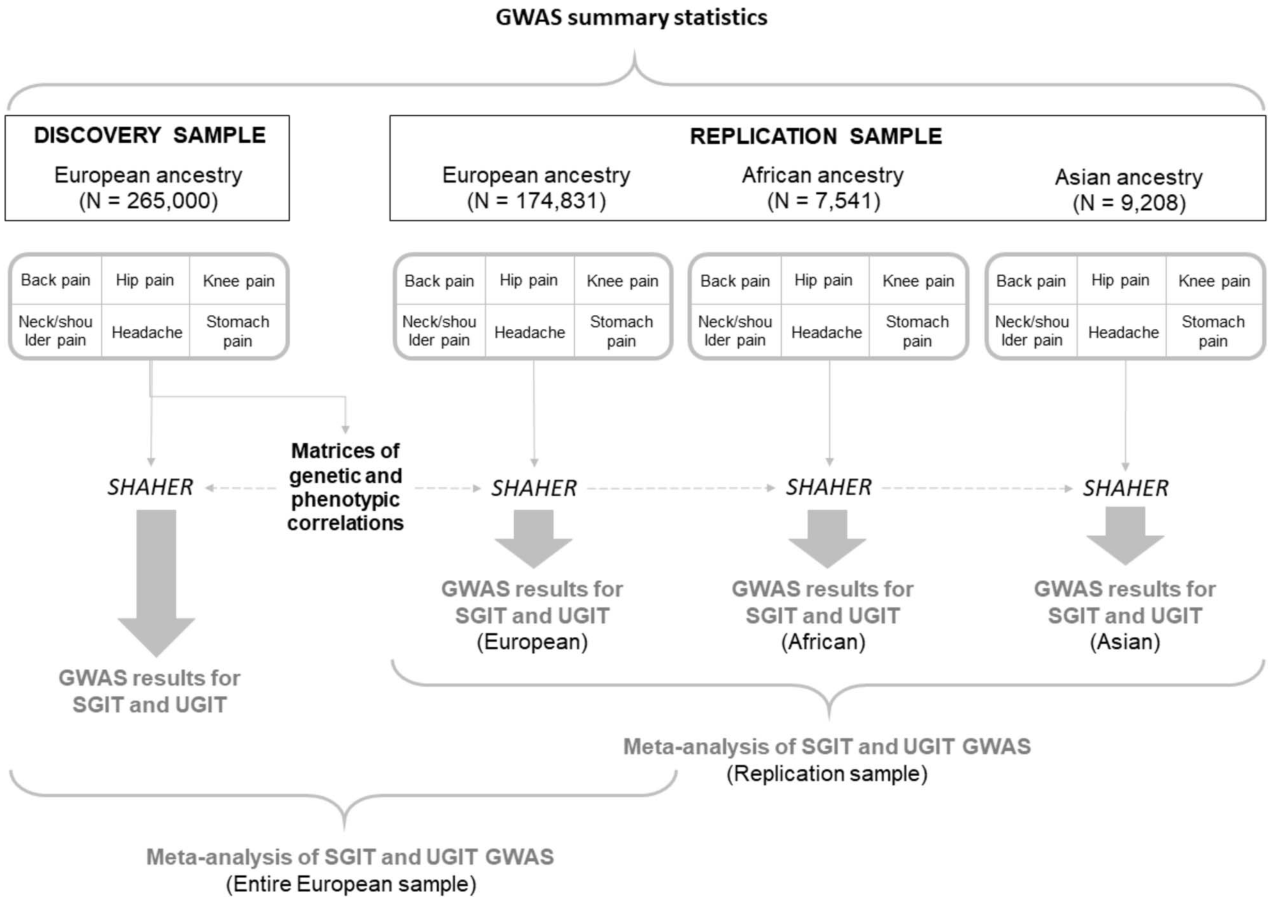

Figure 1. The first step of the study. The black frames label the analyzed sample and the grey frames indicate the input data; the black text in bold shows intermediate results; the text written in grey bold highlights the output data, and the black text written in italic represents the type of analysis.

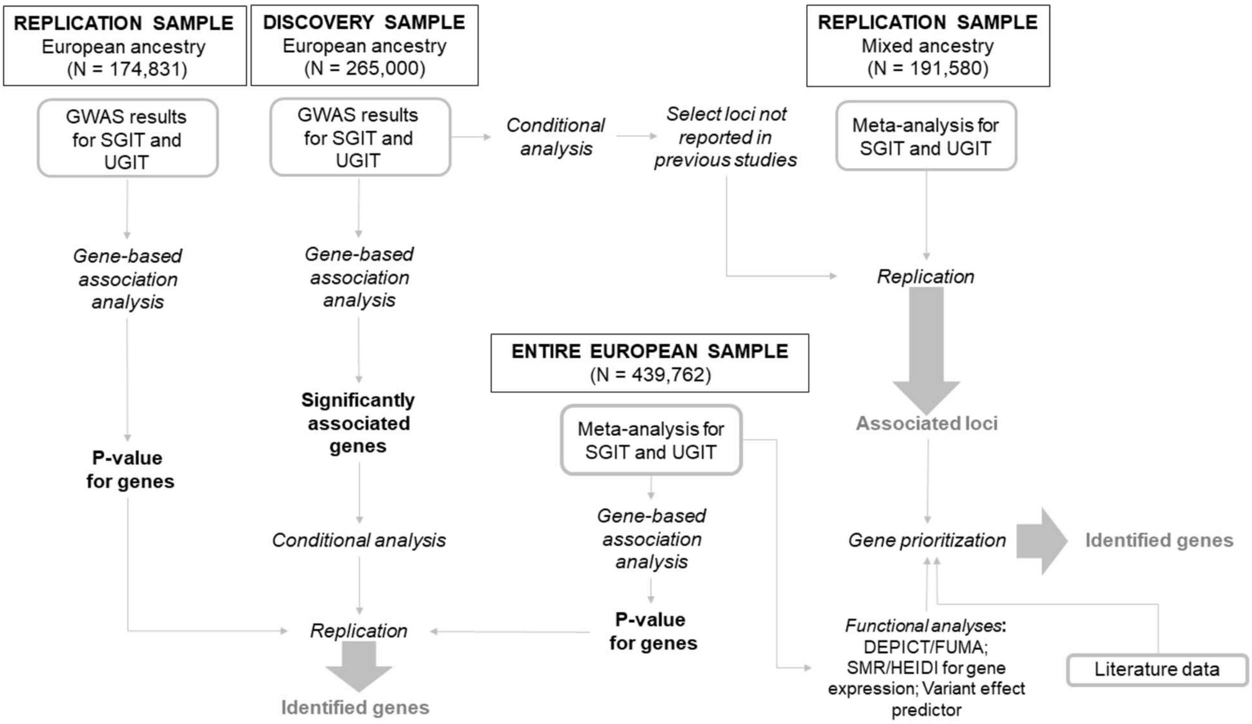
REPLICATION SAMPLE
European ancestry
(N = 174,831)
DISCOVERY SAMPLE
European ancestry
(N = 265,000)
REPLICATION SAMPLE
Mixed ancestry
(N = 191,580)
GWAS results for SGIT and UGIT
GWAS results for SGIT and UGIT
Conditional analysis
Select loci not reported in previous studies
Meta-analysis for SGIT and UGIT
Gene-based association analysis
Gene-based association analysis
Replication
ENTIRE EUROPEAN SAMPLE
(N = 439,762)
Significantly associated genes
Meta-analysis for SGIT and UGIT
Associated loci
P-value for genes
Conditional analysis
Gene-based association analysis
Gene prioritization
Identified genes
Replication
P-value for genes
Functional analyses: DEPICT/FUMA; SMR/HEIDI for gene expression; Variant effect predictor
Literature data
Identified genes

Figure 2. The second step of the study. The black frames label the analyzed sample and the grey frames indicate the input data; the black text in bold shows intermediate results; the text written in grey bold highlights the output data, and the black text written in italic represents the type of analysis.

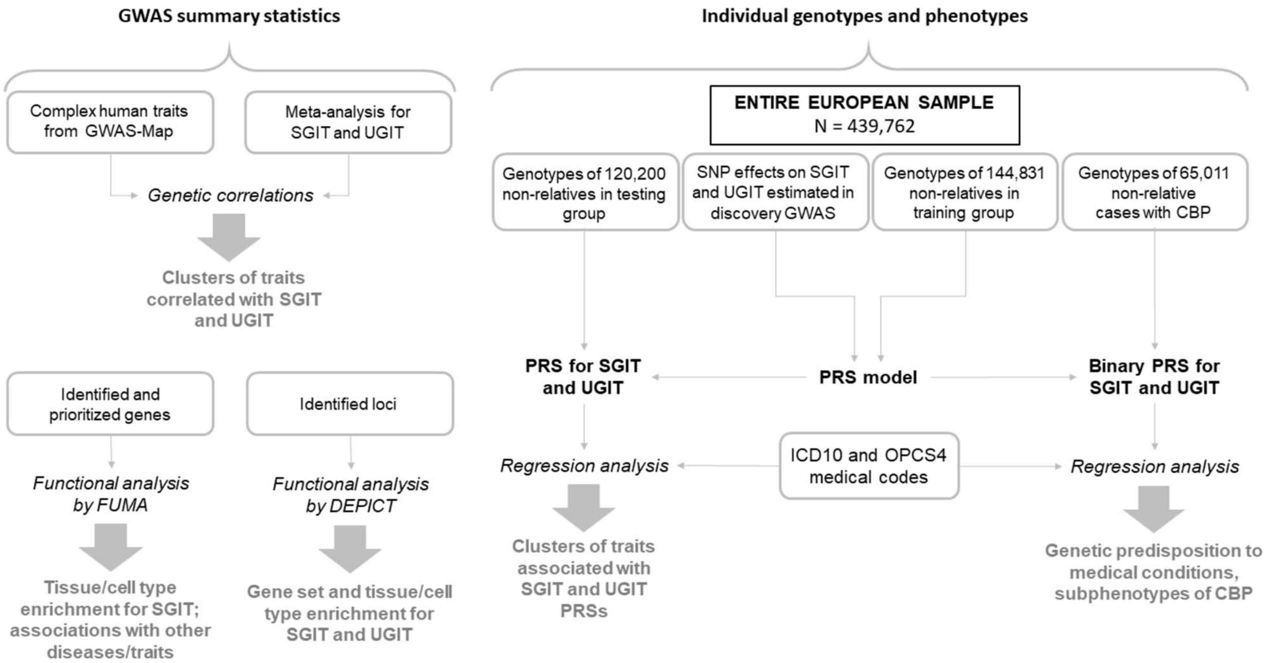
GWAS summary statistics
Complex human traits from GWAS-Map
Meta-analysis for SGIT and UGIT
Genetic correlations
Clusters of traits correlated with SGIT and UGIT
Identified and prioritized genes
Identified loci
Functional analysis by FUMA
Functional analysis by DEPICT
Tissue/cell type enrichment for SGIT; associations with other diseases/traits
Gene set and tissue/cell type enrichment for SGIT and UGIT
Individual genotypes and phenotypes
ENTIRE EUROPEAN SAMPLE
N = 439,762
Genotypes of 120,200 non-relatives in testing group
SNP effects on SGIT and UGIT estimated in discovery GWAS
Genotypes of 144,831 non-relatives in training group
Genotypes of 65,011 non-relative cases with CBP
PRS for SGIT and UGIT
PRS model
Binary PRS for SGIT and UGIT
Regression analysis
ICD10 and OPCS4 medical codes
Regression analysis
Clusters of traits associated with SGIT and UGIT PRSs
Genetic predisposition to medical conditions, subphenotypes of CBP

Figure 3. The third and the fourth steps of the study. The black frames label the analyzed sample and the grey frames indicate the input data; the black text in bold shows intermediate results; the text written in grey bold highlights the output data, and the black text written in italic represents the type of analysis.

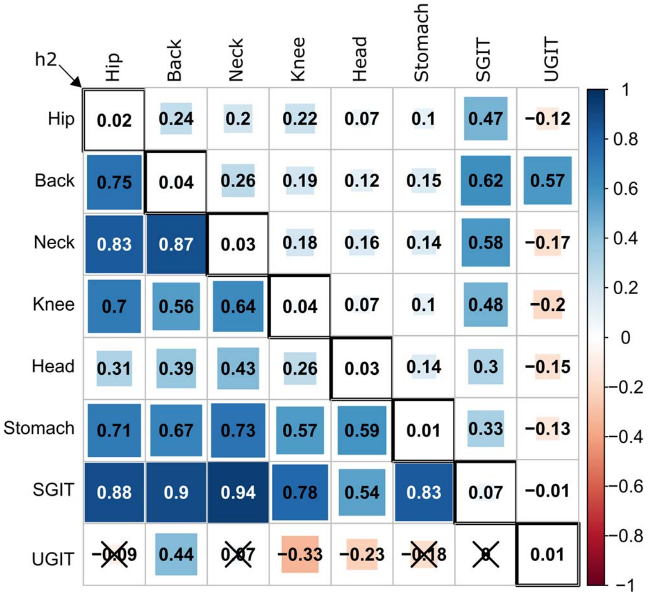

h2	Hip	Back	Neck	Knee	Head	Stomach	SGIT	UGIT
Hip	0.02	0.24	0.2	0.22	0.07	0.1	0.47	−0.12
Back	0.75	0.04	0.26	0.19	0.12	0.15	0.62	0.57
Neck	0.83	0.87	0.03	0.18	0.16	0.14	0.58	−0.17
Knee	0.7	0.56	0.64	0.04	0.07	0.1	0.48	−0.2
Head	0.31	0.39	0.43	0.26	0.03	0.14	0.3	−0.15
Stomach	0.71	0.67	0.73	0.57	0.59	0.01	0.33	−0.13
SGIT	0.88	0.9	0.94	0.78	0.54	0.83	0.07	−0.01
UGIT	~~−0.09~~	0.44	~~0.07~~	−0.33	−0.23	~~−0.18~~	~~0~~	0.01

Figure 4. Heatmap visualization of the heritability, phenotypic correlations and genetic correlations of the original pain traits, SGIT and UGIT. Inscriptions name anatomic sites of chronic pain, UGIT refers to unshared genetic background of CBP. The upper triangle of the matrix represents pairwise phenotypic correlations. The lower triangular of the matrix contains pairwise genetic correlations. Statistically insignificant (P-value > 0.05/28) genetic correlation coefficients are crossed out. Diagonal elements of the matrix correspond to SNP-based heritability (h^2) estimates of the particular traits.

Table ST2a and b). Using these estimates and applying the SHAHER framework, we calculated the coefficients of optimal linear combinations for SGIT and UGIT building (Supplementary Table ST2a) and obtained the summary statistics for SGIT and UGIT. Heritability estimates and correlation coefficients of the original pain traits, SGIT and UGIT are depicted in Fig. 4. Notably, the SNP-based heritability of SGIT is almost two times higher than those of the original traits (0.07 versus 0.01–0.04). The phenotypic and genetic correlations between SGIT and the original traits are higher in comparison to those between the original traits. UGIT shows positive correlation only with CBP.

Gene identification

Identification of loci associated with SGIT and UGIT

The results of SGIT and UGIT GWASs obtained from the discovery sample are visualized at Manhattan and QQ plots (Supplementary Figs 1–4). We identified five loci statistically significantly (P-value < 8.3e-09) associated with SGIT (see Table 1). Conditional analysis showed that each of these loci contains only one independent signal. Four loci (tagged with the following lead SNPs: rs9436127, rs7652179, rs12705966 and rs73581580) were previously observed and replicated in our recent study [16] in the first genetically independent phenotype (GIP1). The locus with the corresponding lead SNP rs11079993 was the new one. Similarly, we identified one locus with rs1271351 as the leading SNP significantly associated with UGIT. Conditional analysis showed a single independent association signal in this region. Since this locus has been already reported in [15], we interpreted it as known. Detailed information on significant loci and their replication is available in Supplementary Table ST3.

Prioritization of genes in the new associated locus

We conducted gene prioritization for the rs11079993 locus associated with SGIT utilizing several approaches: literature-based prioritization of the genes located in this locus; prediction of pathogenicity of SNP effects in the locus using VEP [31], FATHMM-XF [32] and FATHMM-INDEL [33]; DEPICT [34] and FUMA [35] gene prioritization and estimation of pleiotropic effects on gene expression using SMR-HEIDI [36]. Gene prioritization suggested two genes in the rs11079993 locus (see Supplementary Results and Supplementary tables ST4–ST6 for more details): *CA10* (prioritized by literature-based annotation and FUMA) and *LINC01982* (prioritized by literature-based annotation). Although the latter is well studied it provided less evidence for prioritization than *CA10*, so we consider it less likely to be causal. The *CA10* gene may have an effect on chronic pain through processes in the central nervous system, cancer or disease of bones. Despite the fact that *snoZ178* is the nearest gene to rs11079993, it did not provide strong arguments for being causal.

Gene-based association analysis

We performed the gene-based association analysis using different SNP annotation sets within genes. For SGIT we detected 9, 18, and 43 genome-wide significant gene-based signals for nonsynonymous, protein coding and protein non-coding SNP sets, respectively (Supplementary Table ST7). After conditional analysis, 10 out of 43 for non-coding SNP set and one for each coding and non-synonymous SNP sets (both in *SLC39A8*) retained significance. We replicated five of 12 genes using the European replication sample and European meta-analysis (Table 2). For UGIT we detected two significant signals for the non-coding SNP set, and one of them (*CHST3*) passed conditional analysis and replication.

Summary of gene identification

Using prioritization of genes in the associated loci and gene-based association analysis, we identified 18 genes associated with SGIT, with 13 of them being previously reported in our recent works [15, 16] (*SLC39A8, FOXP2, ECM1, AMIGO3, BSN, RBM6, FAM212A, RNF123, UBA7, MIR7114, NSMF, NOXA1, GRIN1*), and 5 of them being new (*CA10, MAML3, TCF20, GABRB2, LINC01982*). One of the identified genes, namely *FOXP2*, was found using both gene prioritization and gene-based analysis. The *SLC39A8* gene was identified using gene-based analysis and has been prioritized in our previous study using the genetically independent phenotype (GIP) approach [16].

For UGIT, we identified the *CHST3* gene utilizing gene-based analysis, and prioritized two genes in the UGIT-associated locus: *CHST3* and *SPOCK2*, failing to give preference to one of them [15].

Analysis of CBP genetic architecture

Gene set and tissue/cell type enrichment

We performed two enrichment analyses based on DEPICT for SNPs associated with SGIT and UGIT in European meta-analysis, and FUMA analysis for the genes identified for SGIT. In DEPICT analysis at P-value < 5e-06 we found SGIT to be enriched in genes involved in the BTBD2 PPI subnetwork and decreased cochlear coiling (Supplementary Table ST8a). We also detected enrichment for genes expressed in the central nervous and neurosecretory systems, retina and neural stem cells (Supplementary Table ST8b). Similar analyses of SGIT-associated variants at P-value < 2.5e-08 threshold provided no significant findings. For UGIT we were able to conduct DEPICT analysis only for SNPs with P-value < 5e-06, but no statistically significant results were obtained. However, we observed a tendency to enrichment for genes expressed in the digestive, nervous, musculoskeletal, cardiovascular, hemic and immune systems.

We did not obtain statistically significant results in tissue specificity and gene set enrichment analyses using FUMA, however, we have shown that SGIT-associated genes have different expression patterns. For instance, there is a group of genes (*NSMF*, *PTBP1*, *RBM6*, *IP6K1*, *UBA7*, *ECM1*, *NOXA1*, *RNF123*) expressed almost in every organ, and a group of genes expressed predominantly in the brain (*GRIN1*, *GABRB2*, *GRM3*, *BSN*, and *CA10*)

Table 1. Loci associated with SGIT and UGIT.

Trait	Lead SNP	Chr:position	RefA/EffA	Nearest gene	Discovery sample				Replication meta-analysis		
					β	se	P-value	EAF	β	se	P-value
SGIT	rs9436127	1:150490565	G/A	*ECM1*	−0.018	0.003	1.72e-10	0.40	−0.012	0.003	5.98e-04
	rs7652179	3:49808618	T/A	*AMIGO3*	0.023	0.004	2.30e-10	0.18	0.011	0.004	1.00e-02
	rs12705966	7:114248851	G/A	*FOXP2*	0.017	0.003	6.55e-09	0.67	0.011	0.004	2.16e-03
	rs73581580	9:140251458	G/A	*EXD3*	0.026	0.004	1.29e-09	0.12	0.029	0.005	5.36e-09
	rs11079993	**17:50301552**	**T/G**	***snoZ178***	**−0.017**	**0.003**	**4.98e-09**	**0.62**	**−0.013**	**0.003**	**7.94e-05**
UGIT	rs1271351	10:73798873	T/C	*CHST3*	−0.018	0.003	1.13e-10	0.43	−0.014	0.003	3.40e-05

The new replicated locus is shown in bold. Other associations were observed in previous studies [15, 16]. Lead SNP—the SNP with the lowest *P*-value in the locus; Chr:position—genomic coordinates in a format "chromosome number: base pairs" (according to the GRCh37 genomic build); RefA—reference (not effective) allele; EffA—effective allele; *β*—effect size of SNP counted for effective allele; se—standard error of *β*; *P*-value—*P*-value of association between SNP and a trait after correction for genomic control; EAF—effective allele frequency.

Table 2. Results of gene-based association analysis of SGIT and UGIT.

Trait	Gene	Chr	Position	SNP set	Gene-based *P*-value			
					Discovery sample	Conditional analysis	European replication sample	European meta-analysis
UGIT	***CHST3***	10	71 964 395	ncod	7.81e-08	7.81e-08[a]	**1.42e-06**	**7.93e-13**
SGIT	***SLC39A8***	4	102 251 080	nsyn	5.68e-10	5.68e-10[a]	**4.73e-09**	**4.38e-17**
	SLC39A8	4	102 251 080	cod	1.17e-07	1.17e-07[a]	**1.62e-06**	**2.54e-13**
	IP6K1	3	49 724 294	ncod	1.32e-10	1.32e-10[a]	0.0083	**2.66e-12**
	GRM3	7	86 643 909	ncod	1.66e-07	1.66e-07[a]	0.0935	**6.55e-08**
	FOXP2	7	114 086 327	ncod	2.00e-07	2.00e-07[a]	**7.90e-04**	**8.22e-11**
	MAML3	4	139 716 753	ncod	3.17e-07	3.17e-07[a]	**6.40e-05**	**1.30e-12**
	PTBP1	19	797 075	ncod	3.64e-07	3.64e-07[a]	0.8760	**2.33e-07**
	TCF20	22	42 160 013	ncod	1.93e-06	1.93e-06[a]	**3.77e-04**	**8.44e-10**
	SOX6	11	15 966 449	ncod	2.01e-06	2.01e-06[a]	0.0921	**4.17e-07**
	FZD10	12	130 162 459	ncod	2.03e-06	2.22e-06	0.2626	4.36e-06
	ERICH2	2	170 766 878	ncod	2.25e-06	2.25e-06[a]	0.1304	3.19e-05
	GABRB2	5	161 288 429	ncod	2.08e-06	2.40e-06	**5.20e-05**	**3.69e-11**

The significance threshold for replication sample was set at *P*-value < 4.2e-03 = 0.05/12, where 12 is the number of genes retained significance after the conditional analysis. [a]These genes harbored SNPs with the lowest *P*-values within 5 Mb from their borders, thus no conditional SNPs were selected, and the gene-based *P*-values remained unchanged.

(Supplementary Fig. 5). These findings are in line with those obtained for SGIT loci utilizing DEPICT. FUMA extends DEPICT findings for SGIT, by accounting for genes identified in gene-based analysis as well and providing more detailed information on expression of particular genes.

Genetic correlation between SGIT, UGIT and complex traits

We estimated the genetic correlation between each of SGIT and UGIT and 730 complex human traits from the GWAS-Map database. SGIT was statistically significantly genetically correlated with almost all of the 322 preselected complex traits, and UGIT provided significant correlations with only 14 of them (see Supplementary Table ST9). In total we grouped all traits in 11 clusters (see Supplementary Table ST9, Fig. 5). There were some distinctions between SGIT and UGIT correlation patterns. First, UGIT was significantly correlated with sitting height which represents the length of the spine, and the second, third and fourth genetically independent phenotypes (GIP2–4) from our recent study [16], while SGIT was not (Supplementary Table ST9). Second, SGIT had a positive direction of genetic correlation with self-reported chronic knee pain and headache, when UGIT was negatively correlated with them. Regardless of statistical significance, SGIT and UGIT demonstrated opposite patterns of genetic correlation (see Fig. 5). While SGIT was mostly positively correlated with traits from such clusters as: respiratory illness and smoking, injuries, socio-economic and family status, psychometric traits, osteoarthritis and other musculoskeletal disorders, UGIT tended to be inversely correlated with these clusters of traits.

Polygenic risk score for SGIT and UGIT. Their role in disease/medical intervention prediction

We developed a model of PRS estimation using a training sample. For a testing sample, we calculated SGIT and UGIT PRSs using individual genotypes. Then we examined association between these PRSs and medical codes available for members of testing sample (see Supplementary Table ST10). We detected 92 ICD10 codes and 57 OPCS4 codes statistically significantly associated with at least one of the studied PRSs. SGIT PRS was associated with all of them. ICD10 codes associated with SGIT and/or UGIT PRSs related to a wide range of disorders, such as disorders of musculoskeletal, nervous, cardio-vascular, digestive and excretory systems, metabolic and skin disorders, diabetes, respiratory and neurological diseases (Supplementary Table ST10, Fig. 6). The associated OPCS4 codes represented mostly surgical manipulations on joints and bones and diagnostic endoscopic examination of gastrointestinal and upper respiratory tract. Also, we observed SGIT PRS to be associated with all of the chronic pain phenotypes and these associations were characterized by the lowest *P*-values (Supplementary Table ST10). Unlike SGIT PRS, UGIT PRS provided only three significant associations, which had been detected for SGIT PRS as well: associations with chronic back and knee pain and with A52 OPCS4 code denoting therapeutic epidural injection, which is due to the association with chronic back pain (Supplementary Table ST10, Fig. 6).

CBP subphenotyping among people with CBP

We investigated the potential of SGIT and UGIT binary-coded PRSs for CBP subphenotyping using only the 65 011 participants with CBP. For each individual and each of two traits, SGIT and UGIT, we formed two types of binary-coded PRSs defined by the lowest and highest deciles of risk (see “Polygenic risk score calculation” in Supplementary Methods section). Then we performed an analysis of associations between each of the four binary-coded PRSs (with two reflecting the lowest decile of the PRS for SGIT and UGIT, respectively, and the other two reflecting the highest decile- for each of SGIT and UGIT) and the ICD10/OPCS4 medical codes and identified 69 ICD10 and 35 OPCS4 codes statistically significantly associated with at least one of binary-coded PRSs (Supplementary Table ST11).

Being in the lowest decile of the SGIT PRS (low genetic predisposition to CBP through shared genetic background) provided a ‘unique’ (not observed for other binary PRS traits) negative association with acute myocardial infarction (I21 ICD10 code, OR = 0.60, *P*-value = 1.09e-06). At the same time, the lowest decile of UGIT PRS (low genetic predisposition to CBP through the unshared genetic background) was uniquely positively associated with unspecified diabetes mellitus (E14 ICD10 code, OR = 1.64, *P*-value = 3.05e-05).

The highest decile of the SGIT PRS (high genetic predisposition to CBP through the shared genetic background) showed 102 statistically significant positive associations with the rest medical

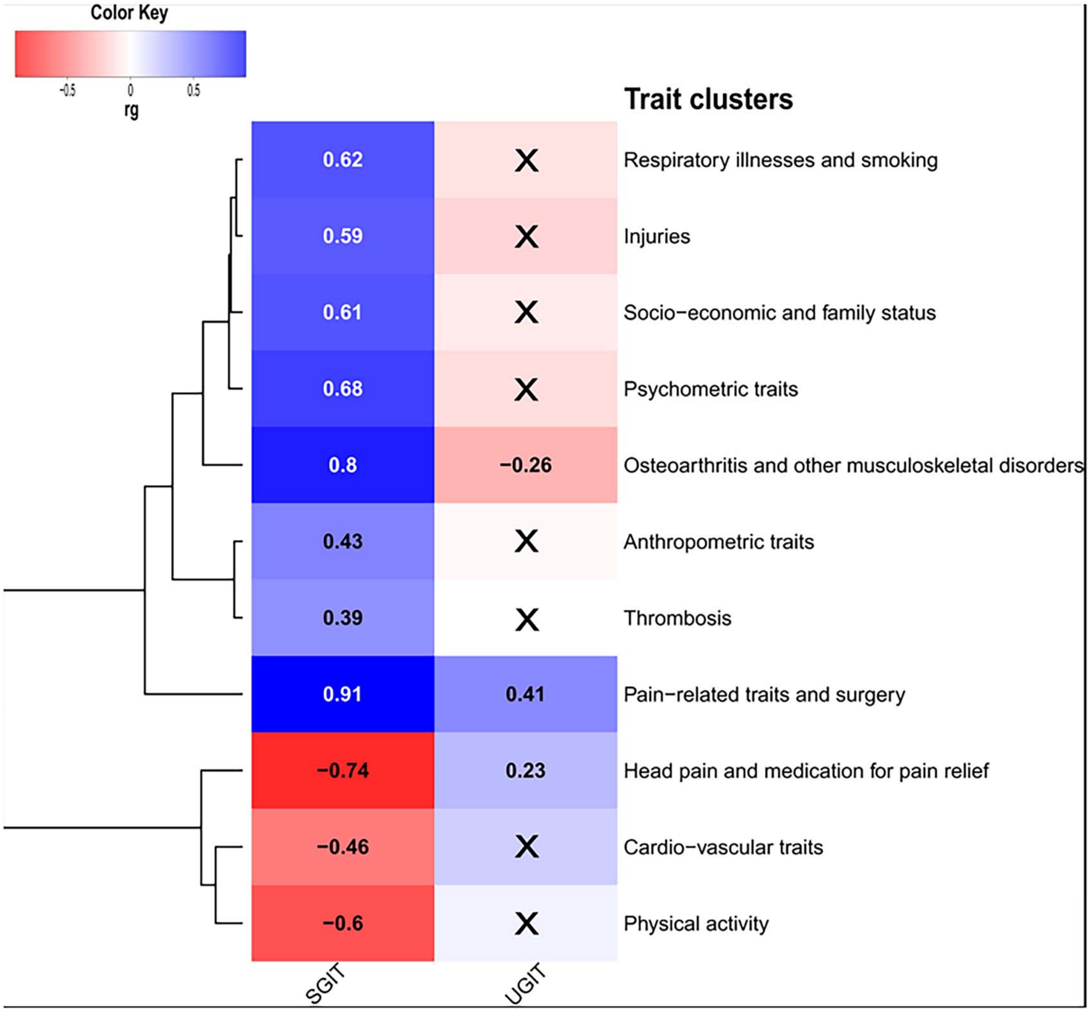

Figure 5. Genetic correlation of SGIT and UGIT with complex human traits. Only 322 traits providing statistically significant genetic correlations (*rg*) with either SGIT or UGIT and *rg* magnitude greater than 0.25 were considered. These traits were grouped into 11 manually annotated clusters. From each cluster we selected one trait (top-trait) providing the smallest *P*-value of genetic correlation among all pairwise correlations with SGIT and UGIT within this cluster and depicted this value on a heatmap. Genetic correlations not passing the significance threshold of *P*-value < 9.41e-07 are crossed out.

codes and 57 of them were associated only with this binary PRS trait. Among these 57 associated codes were those related to diagnostic endoscopic examination of joints and rheumatoid arthritis, surgical manipulation on muscles, joints and bones (such as repair of muscle, bone excision, replacement of joint etc.), conditions of the spine and nervous system, disorders of digestive, genitourinary and endocrine systems and neurological disorders. No specific association was found with the highest decile of the UGIT PRS, but differences in association pattern from other binary PRS traits were found. For example, the SGIT PRS was positively associated with gastrointestinal tract examination procedures (may be because these people are generally prone to pain, so they have unexplained abdominal pain as well or they may take NSAIDs), obesity, arthrosis of knee and hip, and knee surgery, while the UGIT PRS was negative associated with these traits.

Generally, the lowest decile of SGIT PRS and the highest decile of UGIT PRS manifested protective effects on medical states being diagnosed and treated, whereas the lowest decile of UGIT PRS and the highest decile of SGIT PRS had the opposite effect (Supplementary Table ST11).

Discussion

In this work, we first applied the decomposition of genetic background of CBP into shared and unshared ones and showed that they differ in their functions. The shared genetic background is common to different chronic pain conditions while the unshared genetic background is related only to CBP. We built two traits, SGIT and UGIT, corresponding to the shared and unshared genetic background, respectively, and analyzed their properties.

Genes associated with SGIT and UGIT

We identified five loci associated with SGIT and one locus related to UGIT. Among them, only one was new—the locus on chromosome 17 associated with CBP through SGIT. We prioritized two genes (*CA10* and *LINC01982*) near it which are potentially involved in brain development, synapse formation and carcinogenesis, and found associations with gastroesophageal reflux, bone disease, multisite chronic pain and various known risk factors of chronic back pain (educational attainment, smoking, depression). The other four loci found associated with SGIT had previously been reported for GIP1 [16], as expected given our assumption that

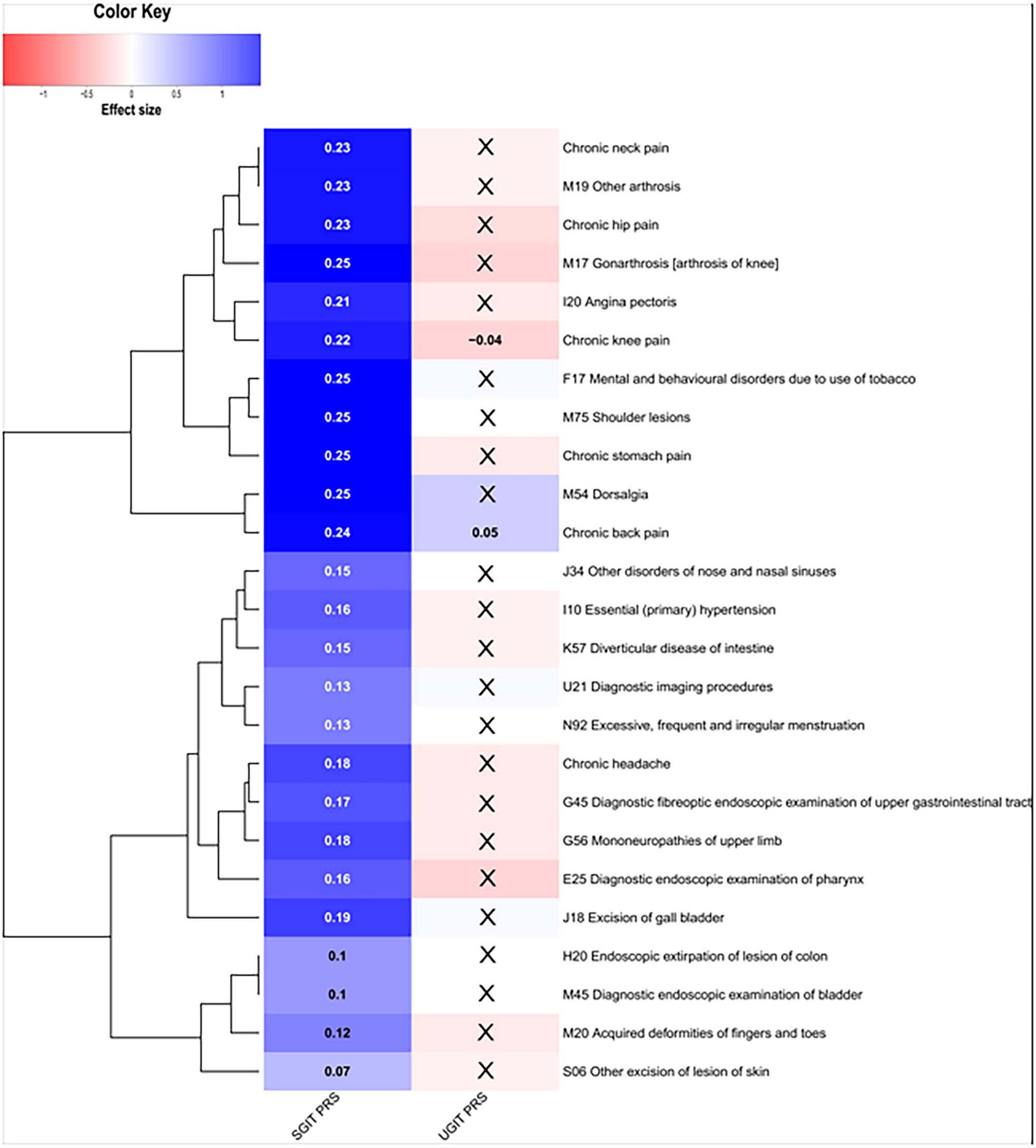

Figure 6. Associations of SGIT and UGIT PRSs with ICD10 and OPCS4 codes and chronic pain phenotypes. Only 92 ICD10 and 57 OPCS4 codes providing statistically significant associations with either CBP, SGIT or UGIT PRS were considered. Medical codes were grouped into 19 clusters. From each cluster we selected one code providing the smallest *P*-value of association with PRSs and depicted its effect sizes on a heatmap. Associations not passing the significance threshold of *P*-value < 8.25e-05 were crossed out.

GIP1 is an approximation of the shared genetic background of the four chronic pain phenotypes studied before. In past work, we have prioritized 12 genes (*MIR7114*, *NOXA1*, *GRIN1*, *NSMF*, *FOXP2*, *BSN*, *AMIGO3*, *RBM6*, *FAM212A*, *RNF123*, *UBA7*, *ECM1*) in these four loci associated with SGIT, with six of them (*NOXA1*, *GRIN1*, *NSMF*, *FOXP2*, *BSN*, *AMIGO3*) being related to the nervous system (brain development and recovery, synapse plasticity, signal transduction, neuropathic and inflammatory pain). Some other genes were related to musculoskeletal (*MIR7114* and *ECM1*, functional in osteoarthritis and osteogenesis, respectively) and immune (*UBA7*) system processes.

In addition to five loci significantly associated with SGIT, there were four more loci suggestively associated (*P*-value < 8.3e-08) with SGIT (Supplementary Table ST12). Among these four loci there was a locus of *SLC39A8* gene reported in our previous study of GIP [16] and there was one new replicated under *P*-value < 8.3e-08 threshold locus on chromosome 13 with the lead SNP rs2587363, located in the *AL356295.1* gene

(Supplementary Fig. 6). We cannot consider this novel locus as statistically significant in the present study, however, it may nevertheless be a target for further investigation. This locus has been reported as associated with multisite chronic pain in females [37], major depressive disorder, osteoarthritis, post-traumatic stress disorder [38, 39], and chronic fatigue syndrome [40]. Moreover, this locus contained polymorphism rs2587363 that was classified as pathogenic according to the FATHMM-XF (Supplementary Table ST13) and demonstrated a pleiotropic effect on the *OLFM4* gene expression (Supplementary Table ST14) in peripheral blood. This gene encodes olfactomedin 4, which is an antiapoptotic factor promoting tumor growth.

Additionally, we performed gene-based association analyses and identified five genes (*SLC39A8, FOXP2, MAML3, TCF20, GABRB2*) significantly associated with SGIT. As can be seen, *FOXP2* was observed in this study both in GWAS and in the gene-based analysis. The *SLC39A8* gene has been reported and replicated for GIP1 [16]. The product of the *SLC39A8* gene is a metal transporter with a role in manganese (Mn) homeostasis, and the missense rs13107325 in this gene is among the top pleiotropic SNPs identified in GWAS. Specifically, it has previously been associated with increased risk of osteoarthritis [41] and severe adolescent idiopathic scoliosis [42]. The gene is known to be mutated in congenital disorder of glycosylation, *SLC39A8*-CDG, with clinical features including osteopenia, broadened long bone epiphysis and joint hypermobility [43, 44]. The dietary manganese deficiency is known to lead to bone and connective tissue disease in animals [45]. *MAML3* has been shown to contribute to several pathways significantly associated with CBP [46]. This gene enables transcription coactivator activity; it is involved in the Notch signaling pathway and positive regulation of transcription by RNA polymerase II. *GABRB2* encodes a GABA (gamma-aminobutyric acid) type A receptor beta subunit. The gene has a pivotal role in the central nervous system and associates with various neuropsychiatric disorders [47]. *TCF20* encodes a transcription factor that recognizes the platelet-derived growth factor-responsive element in the matrix metalloproteinase 3 promoter. The encoded protein is thought to be a transcriptional coactivator, enhancing the activity of transcription factors such as JUN and SP1. Mutations in this gene are associated with autism spectrum disorders (according to NCBI-RefSeq https://www.ncbi.nlm.nih.gov/gene?Db=gene&Cmd=DetailsSearch&Term=6942). Recently, it has been shown that *TCF20* is essential for neurogenesis during embryonic brain development in mouse. *TCF20* dysfunction leads to deficits in neurogenesis, which further results in the development of autism spectrum disorders [48].

Recently, more attention has been paid to the study of the role of rare genetic variants in the control of different traits. In the current study, we also tested the association of SGIT with exome sequencing data from UK Biobank (Supplementary Methods) and performed gene-based association analysis, which identified the *SLC13A1* gene (Supplementary Table ST15a and b). The effect of this gene was explained by its loss of function (LoF) and missense variants. The *SLC13A1* gene has been previously detected as associated with back pain-related traits due to LoF variants [14, 49]. This gene encodes a protein that functions as a high-affinity sodium-dependent sulfate transmembrane transporter [50]. A deficiency of the SLC13A1 protein is associated with a reduced blood sulfate level, which plays a key role in the underlying processes leading to painful intervertebral disc disorders [14]. The association of a gene with disease through LoF variants presents several advantages as a drug target because it provides a clear functional link, target specificity, potential for gene therapy, predictive value, and personalized medicine opportunities. Until now, this gene has been considered as a potential target for treatment against back pain. In the light of our results, *SLC13A1* can be considered as a potential target for treatment against chronic pain irrespective of location.

For UGIT, the *SPOCK2* and *CHST3* genes were detected using both gene-based and gene prioritization analysis. The association of *SPOCK2 with* back pain has been described previously [15]. This gene is located close to carbohydrate sulfotransferase 3 (*CHST3*) which codes for an enzyme that catalyzes proteoglycan sulfating and has been identified as a susceptibility gene for lumbar disc degeneration [51]. The association of *CHST3* with back pain-related phenotypes has also been described [14]. This gene can be considered as most probably causal for back pain in this region, since cumulative evidence L2G scores for *CHST3* and *SPOCK2* are 0.81 and 0.23, respectively, https://genetics.opentargets.org/study-locus/NEALE2_6159_4/10_72001257_A_G, [52].

Many of the genes identified for SGIT have been previously reported in other large-scale studies of various pain phenotypes. In particular, in a recent study [53] analyzing 24 chronic pain traits utilizing another multi-trait approach called Genomic SEM [54], eight out of 18 genes reported for SGIT in present study (*FOXP2, BSN, RBM6, FAM212A, RNF123, UBA7, MAML3, CA10*) were mapped, as well as *OLFM4* gene related to the locus of rs2587363 suggestively associated with SGIT. In a study of multisite chronic pain [13], where the phenotype was defined as a number of anatomic sites with persisting pain (ranging from 0 to 7), six of the SGIT-associated genes were observed (*FOXP2, AMIGO3, SLC39A8, MAML3, ECM1, GABRB2*). Finally, in a study of pain intensity [55] *FOXP2, AMIGO3, SLC39A8, MAML3* and *TCF20* were reviled. Unlike the other two studies mentioned in this paragraph, this one was conducted in a multi-ancestry sample from Million Veteran Program, rather than in a sample of European ancestry individuals from UK Biobank, and included replication. Thus, our findings for SGIT are in line with the results of existing studies utilizing alternative multi-trait methods, samples and pain phenotypes. Notably, no one of the genes related to UGIT were reported in the mentioned publications.

Interestingly, some of the identified genes were studied in animal models. For instance, the effects of *GRIN1* gene on pain development after nerve lesion in mice were reported [56, 57]. Another study in mice reported the role of *ECM1* in chondrocyte differentiation and disorders of cartilage development and endochondral bone formation [58].

Information on genes associated with SGIT is potentially useful in terms of discovering biomarkers and developing multi-target drugs against chronic pain at several anatomic sites at once, because these genes are most likely involved in the development of chronic pain in general. In contrast, genes related to the unshared genetic background of CBP may be more pertinent to the development of chronic pain at back precisely, probably by affecting chondrogenesis or degenerative processes in spine. So UGIT associated genes may be of interest for the development of drugs for treatment of chronic pain specifically in the back.

Gene set and tissue/cell type enrichment of SGIT and UGIT

Based on enrichment analysis and functional annotation of associated loci, the shared genetic background common to different chronic pain conditions contributes to these phenotypes in general through processes in the central nervous and neurosecretory systems. SGIT genetic correlations provided evidence of genetically predisposed psychosocial aspects of CBP. The SNP-based heritability for UGIT was much smaller than that of SGIT, resulting in much less statistical power for all analyses. However, we still detected some significant results. A few findings from functional annotation demonstrated that UGIT was inversely associated with knee pain and headache and positively associated with back pain and medical treatments for back pain such as epidural injection. UGIT also tended to be negatively correlated with respiratory illnesses, musculoskeletal disorders and injuries, demographic parameters and psychometric disorders, whereas SGIT is positively associated with all of these traits. These findings taken together support that the unshared genetic background of CBP may determine the development of pain in the back specifically, whereas the shared genetic background controls non-specific pain manifestations and processes accompanying different pain conditions.

Genetic correlations and polygenic risk scores of SGIT and UGIT

Genetic correlation analysis and PRS analysis are two ways to investigate the influence of genetic background of CBP. Although the lists of the traits included in these analyses overlap, there are many traits presented only in one of them. Thus, genetic correlation analysis adds information on association with self-reported and anthropometric traits (e.g. UGIT is significantly correlated with height), and PRS analysis provides more information on medical diagnoses and interventions (for instance, both SGIT and UGIT PRSs are positively associated with therapeutic epidural injection). Findings from the two methods complement each other. For example, genetic correlation analysis of SGIT reveals genetic predisposition to greater alcohol intake and smoking, and in PRS analysis, we observe its association with mental disorders due to alcohol intake and smoking. Similarly, SGIT analysis shows positive genetic correlation with toothache, and PRS analysis highlights association with tooth removal. For group of traits included in both analyses (such as lower respiratory and urinary system disorders, anxiety and depression, intestine and cardiovascular diseases, sleep and eye disorders, arthritis, spine and knee problems, etc.) results suggest positive association with SGIT in both methods, but they should not be interpreted in the same way. While genetic correlation analysis provides information on pleiotropic effects or linkage in genome [59], PRS analysis reveals associations between the genetic background of CBP and phenotypic traits that can be explained not only by linkage or pleiotropic effects of genes, but also by causal effects of CBP on other traits. Comparing results of genetic correlation analysis with those obtained from PRS analysis can tell us more about probable reasons of observed association between two phenotypes [60]. For instance, when we observe modest genetic correlation between traits along with high magnitude of regression coefficient from PRS analysis, we may speculate that this indicates the role of causal or confounding effects, rather than effects of genetic pleiotropy or linkage. Although this hypothesis has not been properly tested in the studies yet, we still can suppose that trait pairs with such a pattern may be an interesting subject for further studies utilizing Mendelian randomization. For example, we observed this pattern for SGIT and several traits, including obesity (*rg* with BMI was 0.31, beta from PRS analysis for obesity was 0.25), diabetes (*rg* was approximately 0.31 for set of related traits, PRS beta = 0.21), and migraine (*rg* = 0.37, PRS beta = 0.22). Causal effects of increased BMI on back pain, and back pain on type II diabetes, have already been reported in our studies [61, 62], while the association between back pain and migraine is yet to be examined. This link is also interesting to study, since BMI is supposed to affect both back pain [61] and migraine [63, 64]. In contrast, if the magnitude of pairwise genetic correlation coefficient is quite high it is likely that the phenotypic association between two traits is explained by similarity of their genetic background and not by causality. For pairs of traits with these characteristics, information on the similarity of underlying genetic mechanisms can be valuable for development or repurposing of medications affecting both traits via the same pathway. From this prospective, further in-depth studies of the high genetic correlation between irritable bowel syndrome and SGIT (*rg* = 0.78) might be worthwhile.

CBP subphenotypes

The results of genetic analysis of SGIT and UGIT allowed us to estimate their polygenic risk scores for participants with CBP and show that they are associated with different ICD10 and OPCS4 coded conditions. We introduced the binary-coded PRSs for SGIT and UGIT to characterize low and high genetic risk of CBP related to its shared and unshared genetic background, respectively. We showed that these binary-coded PRSs can be potentially helpful for subphenotyping of individuals with CBP, because participants with low or high genetic risk of CBP defined by the shared or unshared genetic background are characterized with different patterns of association with medical interventions and disorders. This can be crucial for forecasting pain trajectories and choosing an adequate treatment. Low genetic liability to CBP explained by shared genetic background turned out to be protective against diagnosis of acute myocardial infarction (OR = 0.60, *P*-value = 1.09e-06), but low genetic risk of CBP mediated through its unshared genetic background was associated with higher predisposition to unspecified diabetes mellitus (OR = 1.64, *P*-value = 3.05e-05). High PRS of SGIT significantly increased the risk of diverse diseases of musculoskeletal, nervous, digestive, genitourinary and endocrine systems (ORs varying from 1.28 to 2.08). Genetic liability to CBP through shared genetic background also showed positive association with gastrointestinal tract examination procedures, this may be because people are generally prone to pain, so they have unexplained abdominal pain as well or they may take non-steroidal anti-inflammatory drugs, which have side effects on gastrointestinal system. All these results should be interpreted with caution, since negative/positive association between PRS and medical code does not necessarily mean protective/detrimental effect on disease development itself but on the disease being diagnosed. For instance, low OR of myocardial infarction among people with low SGIT PRS could potentially indicate that their low genetic liability to pain regardless of its site (including chest pain) can make myocardial infarction much harder to detect. Such a phenomenon was observed for diabetics, who often do not have chest pain, so their myocardial infarctions do not get diagnosed [65, 66].

Limitations of the study

Our study has some limitations and restrictions. First, the discovery analyses were performed in Northern Europeans, so the obtained linear combination coefficients for SGIT and UGIT cannot strictly be applied to individuals of African and Asian ancestry, included in replication sample. Secondly, both discovery and replication sample were based on UK Biobank participants, which means that other cohorts are needed to perform independent replication of the results. Thirdly, here we refer to UGIT as pertaining to unshared genetic background specific to CBP, however, the SHAHER approach does not necessarily accurately divide the genetic background of the traits, so UGIT may have genetic correlations with some of the other chronic pain traits but not with all of them. Finally, we had limited statistical power in UGIT functional analyses, which resulted in few significant findings. This indicates that larger sample size may be helpful in further studies.

Conclusion

Overall, the current work demonstrates that genetic background of CBP can be split into shared between different pain conditions and specific for CBP background. The former is likely to maintain pain mechanisms and manifestations in general through the central nervous and immune systems, functioning of joints, general processes of bone formation and remodeling, while the latter is responsible for processes specific to back pain. Polygenic risk scores separately accounting for shared and unshared genetic background of CBP identify subphenotypes characterized by different genetic predisposition to a range of medical conditions making them possible tools for prognosis in the healthcare system. Twenty genes prioritized for CBP may provide further opportunities for advances in chronic pain management, such as the discovery of new biomarkers and drug targets for chronic pain regardless of its site and drug targets that are specific to CBP.

Materials and methods

Data description

We used the UK Biobank GWAS data ($N_{total} = 456\,000$) relating to four chronic musculoskeletal pain traits (pain in the back, neck, hip, knee) from our recent work (see [16] for the detailed description of the phenotype definition, sample size and sample characteristics). We obtained the remaining two chronic pain phenotypes (stomach pain and headache) from the same UK Biobank [67] sample and conducted GWAS according to the protocol we have described previously (Supplementary Methods, [16]). For each pain trait we split the whole sample of UK Biobank participants into a discovery (N = 265 000, European ancestry individuals) and a replication sample (three samples of African, N = 7541, South Asian, N = 9208, and European descent individuals, N = 174 831). Details of the samples (size, sex and age structure, pain type prevalence and BMI distribution) are available in Supplementary Table ST1. Data were uploaded to the GWAS-Map database [29, 30] for quality control, unification and further functional analysis of GWAS summary statistics. The same genotype and phenotype data were used for making and testing PRS models.

Decomposition of genetic background of chronic back pain

To decompose the genetic background of CBP we implemented the SHAHER framework [25]. This approach is based on the concept that genetic background of each of the genetically related traits can be decomposed into two parts reflecting common for all traits (shared genetic background) and specific for particular trait background. To identify shared and unshared (or specific) background of CBP, SHAHER composes two new traits: SGIT, which condenses the shared genetic background, and UGIT, which is controlled by specific for CBP genetic background. Both SGIT and UGIT are considered as linear combinations of the original traits with specific coefficients. The coefficients for SGIT are calculated by maximizing the proportion of CBP shared genetic background in SGIT genetic background. To calculate the coefficients for UGIT, we estimated the residual genetic background of CBP after adjustment for SGIT. Using these coefficients and the GWAS summary statistics for all original traits, the GWAS summary statistics for SGIT and UGIT of CBP were calculated.

To estimate the SGIT coefficients we utilized the heritability estimates, phenotypic correlation matrices, and genetic correlation matrices (see details in Supplementary Methods) assessed beforehand for the original pain traits in the discovery sample. Further, we used the coefficients obtained using discovery sample in SHAHER analysis of all replication samples (Fig. 1).

Meta-analysis of GWAS summary statistics using METAL

For both SGIT and UGIT we performed two GWAS meta-analyses: (i) a meta-analysis comprising all replication samples (Replication meta-analysis, $N_{total} = 191\,580$); and (ii) a meta-analysis of two European samples (European meta-analysis, $N_{total} = 439\,831$). The first meta-analysis served as a replication set for the GWAS associations observed in the discovery set, while the second one was utilized for further functional annotation. In a gene-based analysis we utilized European meta-analysis for additional replication of the signals from the discovery sample. All the meta-analyses were conducted using an inverse-variance-weighted approach and fixed-effects model implemented in METAL software, version 2011-03-25 [68].

Gene identification

Loci identification and replication

In order to identify loci statistically significantly associated with either SGIT or UGIT we carried out the conditional and joint analysis using GCTA-COJO software (version 1.90.0beta [69]) on the discovery sample. We chose the following settings: minor allele frequency (MAF) not less than 2e-04; stepwise model selection procedure to select independently associated SNPs; significance threshold (applied to statistics after correction for genomic control using the LD Score regression intercept) *P*-value = 5e-08/6 = 8.3e-09, where the denominator corresponds to the number of analyzed traits (SGIT and UGIT from the current work, as well as four genetically independent phenotypes [GIP1-4] from our recent study [16] which were used for comparison); and ± 5000 kb window for linkage disequilibrium assessment. A linkage disequilibrium matrix was computed using PLINK version 1.9 (https://www.cog-genomics.org/plink/1.9/) using 100 000 randomly selected individuals from the discovery set. Loci associated with either SGIT or UGIT were defined as genomic regions of ±250 kb from the lead SNPs identified in COJO analysis.

For both SGIT-associated and UGIT-associated loci we performed a two-step replication procedure. First, we checked whether associations were observed in previous pain studies. We compared SGIT-associated regions with those reported for the first genetically independent phenotype (GIP1) [16] and collated UGIT-associated signal with results from an earlier back pain GWAS [15]. Loci demonstrating the same direction of the effect in the current and previous studies were considered as *known*. Second, we focused on *new* signals (not reported previously) and examined them in the replication meta-analysis. We assumed new signals to be *replicated* if two criteria were met: 1) association in the replication meta-analysis was statistically significant after Bonferroni correction [70] for multiple testing (*P*-value < 0.05/*n*, where *n* is a number of new loci associated with either SGIT or UGIT); and 2) direction of the effect was the same in the discovery sample and Replication meta-analysis.

Gene prioritization in associated loci

We prioritized genes in the replicated locus using a protocol we have described previously in our work on GIP [16]. For gene prioritization we applied a series of methods including (1) literature-based annotation of all genes within the locus using various databases; (2) prediction of SNP effects in the locus utilizing Ensembl Variant Effect Predictor (VEP) [31], FATHMM-XF [32] and FATHMM-INDEL [33] tools; (3) gene prioritization embedded into Data-driven Expression Prioritized Integration for Complex Traits (DEPICT) software [34], and Functional Mapping and Annotation tool (FUMA) [35]; (4) analysis of pleiotropic effects of the replicated loci on gene expression in various tissue types (see Supplementary Table ST16) using an instrument combining Mendelian randomization (Summary data-based Mendelian Randomization, SMR) with heterogeneity testing (Heterogeneity in Dependent Instruments, HEIDI) [36]. Genes provided more evidence for prioritization were considered as more likely to be causal. Details are available in the Supplementary Methods.

Gene-based association analysis

We conducted a gene-based association analysis of SGIT and UGIT utilizing GWAS summary statistics (z-scores and effect sizes) from three datasets: the discovery sample (N = 265 000), the European replication sample (N = 174 831), and data from the European meta-analysis (N_{total} = 439 831). We preliminarily calculated the matrices of correlations between genotypes of all SNPs within a gene using individual genotypes of non-relatives from the entire European sample of UK Biobank participants (N = 315 599) and the PLINK software v2.00a3.7LM (https://www.cog-genomics.org/plink/2.0/) with options –maf 5e-05—geno 0.02. For replication, we restricted to the European sample because discovery and replication gene-based analyses had to be performed using the same matrix of genotype correlations, which is ancestry-specific. In the discovery sample we set the Bonferroni adjusted significance level [70] for the total number of genes (20 000) at 2.5e-06. We defined two criteria for replication of a gene-based signal: 1) the *P*-value in European replication sample had to be less than 0.05/*k*, where *k* corresponds to the number of statistically significant signals in the discovery sample; and 2) the *P*-value in European meta-analysis had to be less than the *P*-value in the discovery sample. See Supplementary Methods for more details on genomic regions studied, methods of gene-based and conditional analyses.

Analysis of CBP genetic architecture

Gene set and tissue/cell type enrichment

We conducted DEPICT tissue or cell type enrichment analyses for GWAS loci associated with SGIT or UGIT in European meta-analysis. We used DEPICT software, version 1.1 rel194 [34], with default settings. For each of the traits we analyzed two SNP lists: a set of variants associated with the trait under *P*-value < 2.5e-08 significance threshold, and a set of SNPs with *P*-value < 5e-06. The significance thresholds corresponds to those recommended by program developers with correction for multiple testing for two traits applied. Variants were selected using GCTA-COJO instrument with settings described above in "Loci identification and replication" section.

For all genes identified for SGIT we ran the gene set enrichment and tissue specificity analyses utilizing FUMA function GENE2FUNC. As the input data we used: 1) all genes prioritized for SGIT in the GWAS loci (both from the new replicated locus and from the loci previously replicated for GIP1); 2) all genes found in gene-based analysis and replicated in European meta-analysis. We analyzed SGIT-associated genes only, because there were not enough genes identified for UGIT to perform the analysis. The GTEx v8 dataset for 30 general tissues was used for tissue specificity analysis. A set of the input genes was tested against each of the sets of differentially expressed genes (DEG) using a hypergeometric test and Bonferroni multiple testing correction. Statistical significance was determined at an adjusted *P*-value < 0.05. We estimated the overrepresentation of the identified genes in the gene sets of the GWAS catalog. Hypergeometric tests were performed to check if the genes of interest were overrepresented in any of the pre-defined gene sets. In this type of analysis, we used FDR (Benjamini—Hochberg method) for multiple testing correction as was recommended by FUMA. Statistical significance was determined at a q-value < 0.05.

Genetic correlation between SGIT, UGIT and complex traits

We assessed genetic correlations of SGIT and UGIT with 730 complex human traits from the GWAS-Map database using LD Score regression tool embedded in the platform. The detailed protocol of selection of 730 complex traits included in the analysis and the full list of them were provided in a recent study by Timmers *et al.* [71]. For further interpretation we restricted our analysis to 322 complex traits which had statistically significant genetic correlations with SGIT and/or UGIT with magnitude greater than 0.25 (*P*-value < 3.42e-5 = 0.05/(730*2), where 730 represents the total number of complex traits and 2 refers to the number of traits). To simplify the perception and visualization of the results of genetic correlation analysis we performed a hierarchal clustering of 322 complex traits. This was done utilizing the ward.D2 method from the standard hclust() R function on a squared matrix of genetic correlations transformed to the Euclidian distances (as.dist() R function) as described previously by Tsepilov *et al.* [16]. We set the arbitrary threshold of h = 1.8 to cut the dendrogram of hierarchical clustering by height and obtained 11 clusters, each of which was then annotated manually. The full list of 322 traits grouped by clusters is provided in Supplementary Table ST9.

Heatmap visualization of the genetic correlations was made using the heatmap.2() function from the gplots R package, version 3.1.1. From each cluster, we depicted one trait having the lowest *P*-value of genetic correlation among all pairwise correlations with SGIT and UGIT within the cluster. The threshold for statistical significance was *P*-value > 9.41e-07 = 0.05/(51 681 + 730*2), where 51 681 is the number of unique genetic correlation coefficients in the squared matrix for 322 complex traits, and 730*2 is the total number of genetic correlations between SGIT, UGIT and 730 complex traits.

Polygenic risk scores of SGIT and UGIT. Their role in disease/medical intervention prediction

In addition to other functional analyses, we examined the prognostic power of SGIT and UGIT polygenic risk scores (PRS) and assessed their role in disease/medical intervention prediction. We calculated the PRSs for SGIT and UGIT utilizing data from the entire European sample (discovery and European replication samples, N_{total} = 439 762) using a three-step algorithm. We used the SBayesR method [72] and the protocol from our recent work on CBP PRS [24], with some modifications. We divided the entire European sample into a training set (discovery sample, N = 265 000), a validation set (subsample from the European replication sample, N = 30 000), and a test set (the other 144 831 Northern Europeans from the European replication sample). The first set was used to develop PRS models, the second one was used to validate these models in individual-level data and select the optimal models for

SGIT and UGIT, and the last dataset was used to assess quality metrics of the optimal models. At the final step, PRS values were calculated for all individuals from entire European sample using optimal models. More details on PRS calculation available in Supplementary Methods.

When the PRS for SGIT and UGIT were estimated for the entire European sample of 439 831, we normalized the PRS (the variance was taken to 1) and used them in a number of generalized linear models (GLMs) considering PRS as a predictor for a particular trait. List of the traits and corresponding phenotypic data were taken from medical histories and questionnaires obtained from UK Biobank participants of European descent from the test dataset mentioned in the paragraph above, using non-relatives only (N = 120 200). Non-relatives were defined by UK Biobank datafield 22 021 (for more details see https://biobank.ndph.ox.ac.uk/showcase/coding.cgi?id=682).

Medical codes were combined to the second level, meaning that participants with a specific medical code of the second level and/or codes of a lower level (the third and/or the fourth) nested under the second level code were all considered to be cases of the second level medical code (for more information on ICD10 and OPCS4 coding in the UK Biobank see https://biobank.ndph.ox.ac.uk/ukb/field.cgi?id=41202 and https://biobank.ndph.ox.ac.uk/ukb/field.cgi?id=41200). Only ICD10 codes from chapters I-XVII were analyzed, OPCS4 codes from chapters X, Y, Z were excluded, and then the remaining codes were filtered by prevalence (> 0.5% and < 99.5%). The final list of the traits (see Supplementary Table ST10) comprised the six self-reported chronic pain phenotypes (questionnaire-based) considered in the study, 165 ICD10 and 132 OPCS4 medical codes served as proxies for the corresponding diseases/medical interventions. To perform GLM-analyses we used a logistic regression from a standard glm() function in R and included sex, age, batch number and the first ten genetic principal components (PC1-10) provided by UK Biobank as covariates in addition to the PRS predictor. The general formula is the following: medical code ∼ age + sex + batch + PC1 + … + PC10 + PRS. Finally, we filtered out the GLM results not passing the significance threshold of *P*-value < 8.25e-05 = 0.05/(2*(165 + 132 + 6)), where 165 and 132 are the numbers of ICD10 and OPCS4 codes, respectively, 6 is a number of pain traits and 2 corresponds to the number of PRSs. For further heatmap visualization of the significant GLM-results we performed a hierarchical clustering of medical codes based on their phenotypic correlation matrix as described above in the genetic correlation analysis. We set a h = 1.25 threshold for cutting the hierarchical clustering dendrogram by height and defined 19 clusters (see Supplementary Table ST10 for more details). Similarly, for the genetic correlation analysis we selected one medical code from each cluster, which provided the lowest *P*-value of association with SGIT and UGIT polygenic risk scores. Alongside medical codes, representing particular clusters, we added six pain traits to the heatmap plot. The visualization was made as described in the genetic correlation analysis section.

CBP subphenotyping among people with CBP

To investigate the potential of SGIT and UGIT PRSs for back pain subphenotyping, we analyzed only CBP cases from the entire European sample, focusing on non-relatives only (N = 65 011). The decision to switch to the entire European sample instead of working with the test sample only was motivated by the limited statistical power of the test sample. We normalized SGIT and UGIT PRS values and recoded each of the vectors of normalized PRSs as binary traits in two different ways. First, we coded the normalized PRS values as 1 if a participant with back pain was attributed to the lowest decile of the normalized PRS vector for SGIT or UGIT, respectively. Normalized PRS values falling out of this range were coded as 0. By such a coding ("yes/no in the lowest decile of the normalized PRS values for SGIT"; "yes/no in the lowest decile of the normalized PRS values for UGIT") we highlighted individuals with the lowest genetic predisposition to CBP through SGIT and UGIT. Then, we coded as 1 the normalized PRS estimates referring to the highest decile of the SGIT or UGIT PRS distribution, respectively, and coded them as 0 otherwise. In this binary coding ("yes/no in the highest decile of the normalized PRS values for SGIT"; "yes/no in the highest decile of the normalized PRS values for UGIT") we marked individuals with the highest genetic predisposition to CBP through SGIT and UGIT. For each of these binary traits we performed GLM analyses using the model described above. As a dependent variable, we considered ICD10 and OPCS4 codes described above. In this sample of 65 011 non-related participants with CBP we selected 199 ICD10 and 165 OPCS4 codes with prevalence > 0.5% and < 99.5%. The significance threshold for this analysis was set at *P* = 3.43e-05 = 0.05/(4*(199 + 165)), where 4 is the number of binary PRS traits, 199 is the number of ICD10 codes, and 165 is the number of OPCS4 codes.

Acknowledgments

This study was conducted using the UK Biobank Resource (project #18219 and #59345). We thank Dr Alexandra S. Shadrina for providing template for Fig. 1 and Dr Sodbo Z. Sharapov for advices on study design.

Supplementary data

Supplementary data is available at *HMG Journal* online.

Conflict of interest statement: Y. S. A. is a co-owner of PolyKnomics BV. Y. S. A. is a full-time employee of GSK PLC and receives salary and stock options as compensation. Other authors declare no conflict of interest.

Funding

This work was supported by the Russian Science Foundation (grant #22-15-20037) and Government of the Novosibirsk region (E. E. E. and T. I. A.).

Data availability

Full project code is available at https://github.com/ElizavetaElgaeva/BP-SH_project_code. GWAS and EWAS summary statistics for all pain traits along with SGIT and UGIT PRS model weights can be found here (https://mga.icgbio.ru/sgit_ugit_cbp_data/).

References

1. Manchikanti L, Singh V, Falco FJE. *et al.* Epidemiology of low back pain in adults. *Neuromodulation* 2014;**17**:3–10.
2. Vos T, Allen C, Arora M. *et al.* Global, regional, and national incidence, prevalence, and years lived with disability for 310 diseases and injuries, 1990–2015: a systematic analysis for the global burden of disease study 2015. *Lancet* 2016;**388**:1545–1602.
3. Foster NE, Anema JR, Cherkin D. *et al.* Prevention and treatment of low back pain: evidence, challenges, and promising directions. *Lancet* 2018;**391**:2368–2383.

4. Reddy K, Sinha P, O'Kane CM. *et al.* Subphenotypes in critical care: translation into clinical practice. *Lancet Respir Med* 2020;**8**: 631–643.
5. Phillips CJ. Economic burden of chronic pain. *Expert Rev Pharmacoecon Outcomes Res* 2006;**6**:591–601.
6. Loeser JD. Chapter 2 pain as a disease. *Handb Clin Neurol* 2006;**81**: 11–20.
7. Gatchel RJ. The biopsychosocial model of chronic pain. *Clin Insights: Chronic Pain* 2013;5–17. https://doi.org/10.2217/EBO.13.469.
8. Scholz J. Mechanisms of chronic pain. *Mol Pain* 2014;**10**:O15.
9. Crofford LJ. Chronic pain: where the body meets the brain. *Trans Am Clin Climatol Assoc* 2015;**126**:167–183.
10. Battie MC, Videman T, Levalahti E. *et al.* Heritability of low back pain and the role of disc degeneration 53rd annual meeting of the Orthopaedic Research Society paper No: 0317. *Pain* 2007;**131**: 272–280.
11. Junqueira DRG, Ferreira ML, Refshauge K. *et al.* Heritability and lifestyle factors in chronic low back pain: results of the Australian twin low back pain study (the AUTBACK study). *Eur J Pain (United Kingdom)* 2014;**18**:1410–1418.
12. Suri P, Palmer MR, Tsepilov YA. *et al.* Genome-wide meta-analysis of 158,000 individuals of European ancestry identifies three loci associated with chronic back pain. *PLoS Genet* 2018;**14**:e1007601.
13. Johnston KJA, Adams MJ, Nicholl BI. *et al.* Genome-wide association study of multisite chronic pain in UK biobank. *PLoS Genet* 2019;**15**:e1008164.
14. Bjornsdottir G, Stefansdottir L, Thorleifsson G. *et al.* Rare SLC13A1 variants associate with intervertebral disc disorder highlighting role of sulfate in disc pathology. *Nat Commun* 2022;**13**:634.
15. Freidin MB, Tsepilov YA, Palmer M. *et al.* Insight into the genetic architecture of back pain and its risk factors from a study of 509,000 individuals. *Pain* 2019;**160**:1361–1373.
16. Tsepilov YA, Freidin MB, Shadrina AS. *et al.* Analysis of genetically independent phenotypes identifies shared genetic factors associated with chronic musculoskeletal pain conditions. *Commun Biol* 2020;**3**:329.
17. Li S, Brimmers A, Van Boekel RLM. *et al.* Systematic review and meta-analysis a systematic review of genome-wide association studies for pain, nociception, neuropathy, and pain treatment responses. *Pain* 2023;**164**:1891–1911.
18. Vehof J, Zavos HMS, Lachance G. *et al.* Shared genetic factors underlie chronic pain syndromes. *Pain* 2014;**155**:1562–1568.
19. Williams FMK, Spector TD, MacGregor AJ. Pain reporting at different body sites is explained by a single underlying genetic factor. *Rheumatology* 2010;**49**:1753–1755.
20. Jensen RK, Jensen TS, Kjaer P. *et al.* Can pathoanatomical pathways of degeneration in lumbar motion segments be identified by clustering MRI findings. *BMC Musculoskelet Disord* 2013;**14**:198.
21. Ranoux D, Attal N, Morain F. *et al.* Botulinum toxin type a induces direct analgesic effects in chronic neuropathic pain. *Ann Neurol* 2008;**64**:274–283.
22. Tagliaferri SD, Angelova M, Zhao X. *et al.* Artificial intelligence to improve back pain outcomes and lessons learnt from clinical classification approaches: three systematic reviews. *NPJ Digit Med* 2020;**3**:93.
23. Shendure J, Findlay GM, Snyder MW. Genomic medicine-progress, pitfalls, and promise. *Cell* 2019;**177**:45–57.
24. Tsepilov YA, Elgaeva EE, Nostaeva AV. *et al.* Development and replication of a genome-wide polygenic risk score for chronic back pain. *J Pers Med* 2023;**13**:977.
25. Svishcheva G, Tiys E, Elgaeva E. *et al.* A novel framework for analysis of the shared genetic background of correlated traits. *Genes (Basel)* 2022;**13**:1694.
26. Lee S, Wu MC, Lin X. Optimal tests for rare variant effects in sequencing association studies. *Biostatistics* 2012;**13**:762–775.
27. Wang K, Abbott D. A principal components regression approach to multilocus genetic association studies. *Genet Epidemiol* 2008;**32**:108–118.
28. Liu Y, Chen S, Li Z. *et al.* ACAT: a fast and powerful p value combination method for rare-variant analysis in sequencing studies. *Am J Hum Genet* 2019;**104**:410–421.
29. Shashkova TI, Gorev DD, Pakhomov ED. *et al.* The GWAS-MAP platform for aggregation of results of genome-wide association studies and the GWAS-MAP|homo database of 70 billion genetic associations of human traits. *Vavilovskii Zhurnal Genet Selektsii* 2021;**24**:876–884.
30. Shashkova TI, Pakhomov ED, Gorev DD. *et al.* PheLiGe: an interactive database of billions of human genotype-phenotype associations. *Nucleic Acids Res* 2021;**49**:D1347–D1350.
31. McLaren W, Gil L, Hunt SE. *et al.* The Ensembl variant effect predictor. *Genome Biol* 2016;**17**:122.
32. Rogers MF, Shihab HA, Mort M. *et al.* FATHMM-XF: accurate prediction of pathogenic point mutations via extended features. *Bioinformatics* 2018;**34**:511–513.
33. Ferlaino M, Rogers MF, Shihab HA. *et al.* An integrative approach to predicting the functional effects of small indels in non-coding regions of the human genome. *BMC Bioinformatics* 2017;**18**:442.
34. Pers TH, Karjalainen JM, Chan Y. *et al.* Biological interpretation of genome-wide association studies using predicted gene functions. *Nat Commun* 2015;**6**:5890.
35. Watanabe K, Taskesen E, van Bochoven A. *et al.* Functional mapping and annotation of genetic associations with FUMA. *Nat Commun* 1826;**8**:1826.
36. Zhu Z, Zhang F, Hu H. *et al.* Integration of summary data from GWAS and eQTL studies predicts complex trait gene targets. *Nat Genet* 2016;**48**:481–487.
37. Johnston KJA, Ward J, Ray PR. *et al.* Sex-stratified genome-wide association study of multisite chronic pain in UK biobank. *PLoS Genet* 2021;**17**:e1009428.
38. Zhang F, Rao S, Baranova A. Shared genetic liability between major depressive disorder and osteoarthritis. *Bone Joint Res* 2022;**11**:12–22.
39. Zhang F, Rao S, Cao H. *et al.* Genetic evidence suggests posttraumatic stress disorder as a subtype of major depressive disorder. *J Clin Invest* 2022;**132**:e145942.
40. Das S, Taylor K, Kozubek J. *et al.* Genetic risk factors for ME/CFS identified using combinatorial analysis. *J Transl Med* 2022;**20**: 598.
41. Tachmazidou I, Hatzikotoulas K, Southam L. *et al.* Identification of new therapeutic targets for osteoarthritis through genome-wide analyses of UK biobank data. *Nat Genet* 2019;**51**:230–236.
42. Haller G, McCall K, Jenkitkasemwong S. *et al.* A missense variant in SLC39A8 is associated with severe idiopathic scoliosis. *Nat Commun* 2018;**9**:4171.
43. Park JH, Hogrebe M, Grüneberg M. *et al.* SLC39A8 deficiency: a disorder of manganese transport and glycosylation. *Am J Hum Genet* 2015;**97**:894–903.
44. Bonaventura E, Barone R, Sturiale L. *et al.* Clinical, molecular and glycophenotype insights in SLC39A8-CDG. *Orphanet J Rare Dis* 2021;**16**:307.
45. Hidiroglou M, Ivan M, Bryan MK. *et al.* Assessment of the role of manganese in congenital joint laxity and dwarfism in calves. *Ann Rech Vet* 1990;**21**:281–284.

46. Bortsov AV, Parisien M, Khoury S. *et al.* Brain-specific genes contribute to chronic but not to acute back pain. *Pain Rep* 2022;**7**:e1018.
47. Barki M, Xue H. GABRB2, a key player in neuropsychiatric disorders and beyond. *Gene* 2022;**809**:146021.
48. Feng C, Zhao J, Ji F. *et al.* TCF20 dysfunction leads to cortical neurogenesis defects and autistic-like behaviors in mice. *EMBO Rep* 2020;**21**:e49239.
49. Ao X, Parisien M, Zidan M. *et al.* Rare variant analyses in large-scale cohorts identified SLC13A1 associated with chronic pain. *Pain* 2023;**164**:1841–1851.
50. Langford R, Hurrion E, Dawson PA. Genetics and pathophysiology of mammalian sulfate biology. *J Genet Genomics* 2017;**44**: 7–20.
51. Song YQ, Karasugi T, Cheung KMC. *et al.* Lumbar disc degeneration is linked to a carbohydrate sulfotransferase 3 variant. *J Clin Invest* 2013;**123**:4909–4917.
52. Mountjoy E, Schmidt EM, Carmona M. *et al.* An open approach to systematically prioritize causal variants and genes at all published human GWAS trait-associated loci. *Nat Genet* 2021;**53**: 1527–1533.
53. Zorina-Lichtenwalter K, Bango CI, Van Oudenhove L. *et al.* Genetic risk shared across 24 chronic pain conditions: identification and characterization with genomic structural equation modeling. *Pain* 2023;**164**:2239–2252.
54. Grotzinger AD, Rhemtulla M, de Vlaming R. *et al.* Genomic structural equation modelling provides insights into the multivariate genetic architecture of complex traits. *Nat Hum Behav* 2019;**3**: 513–525.
55. Toikumo S, Vickers-Smith R, Jinwala Z. *et al.* A multi-ancestry genetic study of pain intensity in 598,339 veterans. *Nat Med* 2024;**30**:1075–1084.
56. Inquimbert P, Moll M, Latremoliere A. *et al.* NMDA receptor activation underlies the loss of spinal dorsal horn neurons and the transition to persistent pain after peripheral nerve injury. *Cell Rep* 2018;**23**:2678–2689.
57. Yuan BT, Li MN, Zhu LP. *et al.* TFAP2A is involved in neuropathic pain by regulating Grin1 expression in glial cells of the dorsal root ganglion. *Biochem Pharmacol* 2024;**227**:116427.
58. Kong L, Zhao Y-P, Tian Q-Y. *et al.* Extracellular matrix protein 1, a direct targeting molecule of parathyroid hormone-related peptide, negatively regulates chondrogenesis and endochondral ossification via associating with progranulin growth factor. *FASEB J* 2016;**30**:2741–2754.
59. Chebib J, Guillaume F. Pleiotropy or linkage? Their relative contributions to the genetic correlation of quantitative traits and detection by multitrait GWA studies. *Genetics* 2021;**219**:iyab159.
60. Elgart M, Goodman MO, Isasi C. *et al.* Correlations between complex human phenotypes vary by genetic background, gender, and environment. *Cell Rep Med* 2022;**3**:100844.
61. Elgaeva EE, Tsepilov Y, Freidin MB. *et al.* ISSLS prize in clinical science 2020. Examining causal effects of body mass index on back pain: a Mendelian randomization study. *Eur Spine J* 2020;**29**: 686–691.
62. Suri P, Elgaeva EE, Williams FMK. *et al.* Evidence of causal effects of blood pressure on back pain and back pain on type II diabetes provided by a bidirectional Mendelian randomization study. *Spine J* 2023;**23**:1161–1171.
63. Jareebi MA, Lyall DM, Gharawi NF. *et al.* Causal associations of modifiable risk factors with migraine: evidence from Mendelian randomization analysis. *Cureus* 2024;**16**:e53448.
64. Ornello R, Ripa P, Pistoia F. *et al.* Migraine and body mass index categories: a systematic review and meta-analysis of observational studies. *J Headache Pain* 2015;**16**:27–40.
65. Elliott MD, Heitner JF, Kim H. *et al.* Prevalence and prognosis of unrecognized myocardial infarction in asymptomatic patients with diabetes: a two-center study with up to 5 years of follow-up. *Diabetes Care* 2019;**42**:1290–1296.
66. Chiariello M, Indolfi C. Silent myocardial ischemia in patients with diabetes mellitus. *Circulation* 1996;**93**:2089–2091.
67. Sudlow C, Gallacher J, Allen N. *et al.* UK biobank: an open access resource for identifying the causes of a wide range of complex diseases of middle and old age. *PLoS Med* 2015;**12**:e1001779.
68. Willer CJ, Li Y, Abecasis GR. METAL: fast and efficient meta-analysis of genomewide association scans. *Bioinformatics* 2010;**26**:2190–2191.
69. Yang J, Ferreira T, Morris AP. *et al.* Conditional and joint multiple-SNP analysis of GWAS summary statistics identifies additional variants influencing complex traits. *Nat Genet* 2012;**44**:369–375.
70. Curtin F, Schulz P. Multiple correlations and Bonferroni's correction. *Biol Psychiatry* 1998;**44**:775–777.
71. Timmers PRHJ, Tiys ES, Sakaue S. *et al.* Mendelian randomization of genetically independent aging phenotypes identifies LPA and VCAM1 as biological targets for human aging. *Nat Aging* 2022;**2**: 19–30.
72. Lloyd-Jones LR, Zeng J, Sidorenko J. *et al.* Improved polygenic prediction by Bayesian multiple regression on summary statistics. *Nat Commun* 2019;**10**:5086.

Human Molecular Genetics, 2025, Vol. 34, 8, 711–725
https://doi.org/10.1093/hmg/ddae195
Original Article